Vol. 14(2): 317-339, May 2026 DOI: https://doi.org/10.23960/jsl.v14i2.1372

Jurnal Sylva Lestari

P-ISSN: 2339-0913
E-ISSN: 2549-5747

Journal homepage: https://sylvalestari.fp.unila.ac.id

Full Length Research Article

Enhancing Dimensional Stability of Sengon Wood through Synergistic Citric Acid–Glycerol Cross-Linking and SiO_2/TiO_2 Nanocomposite Impregnation

Sartika[1,2], Istie Sekartining Rahayu[1,*], Wayan Darmawan[1], Andi Detti Yunianti[2], Esti Prihatini[1], Gilang Dwi Laksono[1], Rohmat Ismail[3]

[1] Department of Forest Products, Faculty of Forestry and Environment, IPB University, Bogor, Indonesia
[2] Study Program of Forestry Engineering, Faculty of Forestry, University of Hasanuddin, Makassar, Indonesia
[3] Department of Chemistry, Faculty of Mathematics and Natural Sciences, IPB University, Bogor, Indonesia
[*] Corresponding author. E-mail address: istiesr@apps.ipb.ac.id

ARTICLE HISTORY:

Received: 30 November 2025
Peer review completed: 30 March 2026
Received in revised form: 13 April 2026
Accepted: 7 May 2026

KEYWORDS:

Citric acid-glycerol
Dimensional stability
Sengon
SiO_2/TiO_2 nanocomposite
Wood modification

ABSTRACT

Sengon wood (*Falcataria moluccana*) is a fast-growing, low-quality species. In this research, nanoparticle-based impregnation was used to improve the quality and characteristics of sengon wood. SiO_2 nanoparticles derived from bamboo leaves were synthesized using the sol-gel method, while TiO_2 nanoparticles and SiO_2/TiO_2 nanocomposites were synthesized using the hydrothermal method. A mixture of citric acid, glycerol, and nanoparticles (SiO_2, TiO_2, and SiO_2/TiO_2 composite) was formulated as an impregnation solution at 1% concentration. Sengon wood impregnation was conducted using a vacuum-pressure method. The physical properties tested included weight percent gain (WPG), bulking effect (BE), anti-swelling efficiency (ASE), water uptake (WU), and density. The size of the synthesized nanoparticles was analyzed using a particle size analyzer (PSA). The impregnated sengon wood was characterized using Fourier transform infrared spectroscopy (FTIR) to identify functional groups and X-ray diffraction (XRD) to determine the degree of crystallinity. PSA analysis showed that the material used in the impregnation process is nanoscale (< 100 nm) and exhibits the best dispersion stability in the SiO_2/TiO_2 nanocomposite. Nanoparticle-impregnated sengon wood exhibited reduced WU and improved dimensional stability compared to untreated samples, especially in citric acid–glycerol and composite nanoparticle treatments. FTIR analysis identified the formation of ester bonds and the reduction of hydroxyl groups, and XRD analysis showed a decrease in crystallinity upon impregnation with nanoparticles and a citric acid–glycerol mixture. Overall, the use of citric acid–glycerol with the nanocomposite showed effectiveness in improving the dimensional stability and physical properties of sengon wood.

1. Introduction

Environmentally friendly materials such as wood are widely used for various purposes, including construction and furniture. The demand for wood in Indonesia continues to increase every year. According to data from the Central Statistics Agency (BPS), roundwood production increased by 5.52%, from 64.65 million m³ in 2022 (BPS 2022) to 68.22 million m³ in 2023 (BPS 2023). Fast-growing wood currently dominates the wood production industry and has become an

alternative for wood utilization in Indonesia. Sengon wood is a relatively fast-growing species and is therefore widely cultivated and used. Sengon has a harvest cycle of under 10 years (Rahayu et al. 2020), and its specific gravity ranges from 0.24 to 0.49, corresponding to strength and durability classes IV–V (Handayani 2016). However, this fast-growing wood has inferior qualities, such as low resistance to fire, weather, and wood-destroying organisms, which limit its use.

Improving the strength and durability, and extending the service life of wood, can be achieved by modifying the wood as an alternative solution. Currently, the impregnation method is one of the modifications under development to protect wood from external influences (Belchinskaya et al. 2022), as it introduces chemicals into the wood to act as protective agents (Asci and Keskin 2021). Several researchers have utilized this method with various materials. For instance, Rahayu et al. (2021) reported increases in the physical, mechanical, and durability properties of sengon wood using impregnation with a mixture of monoethylene glycol and silicon dioxide (SiO_2) nanoparticles. Similarly, Kacíková et al. (2021) successfully improved the fire resistance of oak wood by combining SiO_2, titanium dioxide (TiO_2), and ZnO nanoparticles with sodium silicate. Additionally, Belchinskaya et al. (2022) showed improved wood resistance to biological and water degradation by utilizing oils.

Moreover, nanoparticle-based materials have accelerated technological developments in the field of wood impregnation. Impregnation with nanoscale particles is more effective because their size is statistically smaller than the pore size of wood (Bossert et al. 2020). Other advantages of using nanoparticles, such as the SiO_2–TiO_2 combination, include enhanced hydrophobicity, photocatalytic properties, and resistance to environmental factors, including humidity and temperature, that accelerate weathering (Liu et al. 2021). Gürgen and Yıldız (2023) also reported the effectiveness of SiO_2 and TiO_2 nanoparticles as impregnation materials for improving wood quality. SiO_2 nanoparticles can be produced from bamboo leaves, a biomass waste. According to Saputra et al. (2017), bamboo leaves contain around 77.96% to 92.56% silica. SiO_2 nanoparticles can improve the surface hardness, dimensional stability, and thermal stability of wood (Bak et al. 2018; Dong et al. 2014; Rahayu et al. 2021). In addition, TiO_2 nanoparticles can improve hardness, fire resistance, density, photocatalytic activity, and resistance to UV radiation and organic pollutants (Garskaite et al. 2019; Liu et al. 2021; Rahayu et al. 2022a).

Beyond improving wood quality, SiO_2 and TiO_2 nanoparticles, when combined, can produce synergistic effects from their respective advantages. However, Horst et al. (2021) explained that TiO_2 nanoparticles tend to agglomerate when immersed in liquid, and accordingly, they may not perform well on wood. This agglomeration can be avoided by the impregnation method. The Mn (3 wt%)/MnO_2 mixture is mixed with SiO_2 to improve dispersion in the step (Rosales and Esquivel 2020). Therefore, a citric acid–glycerol solvent was required to disperse the SiO_2 and TiO_2 nanoparticles used in this study.

Essoua et al. (2016) also explained that the combination of citric acid–glycerol as a solvent for nanoparticles can further increase the hardness and weather resistance of wood and the formation of ester bonds with hydroxy functionalities of cellulose and hemicellulose in wood, so that the nanoparticles that have been dispersed are not easily leached. Rilda et al. (2020) showed that the connector between the TiO_2–SiO_2/chitosan composite nanoparticles and cotton fibers is citric acid, which serves as a binder. On the other hand, glycerol can improve the mechanical properties of materials (Mousa and Taha 2022). Citric acid and glycerol are also categorized as non-biocide chemicals.

As previously mentioned, fast-growing sengon wood is widely used in Indonesia. However, its durability is affected by its high susceptibility to weathering, biological degradation, and fire. Therefore, the novelty of this study lies not in the individual use of SiO_2 or TiO_2 nanoparticles, but in the synergistic integration of a citric acid–glycerol matrix with SiO_2/TiO_2 nanocomposites for the dimensional stabilization of sengon wood (*Falcataria moluccana*), a fast-growing species with limited prior modification studies. This study aims to analyze the potential of combining SiO_2 and TiO_2 nanoparticles with citric acid as a solvent to improve the properties of sengon wood, which has inferior quality.

2. Materials and Methods

2.1. Tools and Materials

The equipment used in this study included a furnace, porcelain dishes, analytical scales, measuring cups, beakers, funnels, ovens, desiccators, calipers, ultrasonicators, magnetic stirrers, and impregnation tubes. The analytical equipment included a particle size analyzer (PSA) (Horiba SZ-100, Horiba, Ltd., Kyoto, Japan), X-ray diffraction analysis (XRD) (SMARTLAB RIGAKU, Rigaku Corporation, Tokyo, Japan), and Fourier transform infrared spectroscopy (FTIR) (Shimadzu IR-Prestige 21, Shimadzu Corporation, Kyoto, Japan).

The materials used in this study were 5-year-old sengon wood (*Falcataria moluccana*) from Sukabumi (West Java), betung bamboo *(Dendrocalamus asper*) leaves from Bogor (West Java) as the precursor for SiO_2 synthesis, titanium dioxide (TiO_2) (100% pure, Pure Supplement), citric acid (99%, Weifang Ensign Industry Co., Ltd.), glycerol (97%, Ecogreen Oleochemicals), NaOH (98%, EMD Milipore Corporation), ethanol (99%, EMD Milipore Corporation), and demineralized water.

2.2. Sample Preparation

The wood used was sengon with a diameter of 28 cm, cut to a length of 100 cm from the base to the branch-free height, and then split into boards. All test samples were obtained from the same tree and cut without distinguishing between sapwood and heartwood (**Fig. 1)**. The dimensions of the test samples are shown in **Table 1**. The test samples were then dried in an oven before impregnation treatment. The oven-dry weight obtained after drying at 103 ± 2 °C to constant mass was used as the reference weight for calculating impregnation uptake. Each test was conducted five times for each treatment (untreated, citric acid–glycerol (CA.G), CA.G–silicon dioxide (S) 1%, CA.G–titanium dioxide (T) 1%, CA.G–composite (C) 1%, and water–composite (C) 1%).

2.3. Synthesis of SiO_2 Nanoparticles

SiO_2 nanoparticles were synthesized using the sol-gel method. Bamboo leaves were sun-dried until dry (light brown in color) and weighed to a total of 1000 g. The dried leaves were then ignited under controlled open-air conditions without the addition of external fuel and allowed to undergo initial combustion for approximately 1 hour until charcoal formation was achieved. The resulting charcoal was weighed and placed in a porcelain container, then burned in the furnace at 700 °C for 6 hours to produce ash. The ash from furnace combustion, weighing up to 1 g, was weighed and mixed with 40 mL of 3 M HCl. After that, the mixture was stirred and heated at 80

°C for 30 minutes using a magnetic stirrer. The mixture was cooled, filtered, and the precipitate was collected. The precipitate obtained was added to 40 mL of 3 M NaOH, stirred and heated at 90 °C for 30 minutes (Cahyani et al. 2022). The filtrate obtained was added to 40 mL of demineralized water and 20 mL of 96% ethanol, and the mixture was stirred until homogeneous (Lu et al. 2017). The white precipitate was filtered, dried at 105 °C for 2 hours, and then calcined at 450 °C for 3 hours (Manchanda et al. 2017).

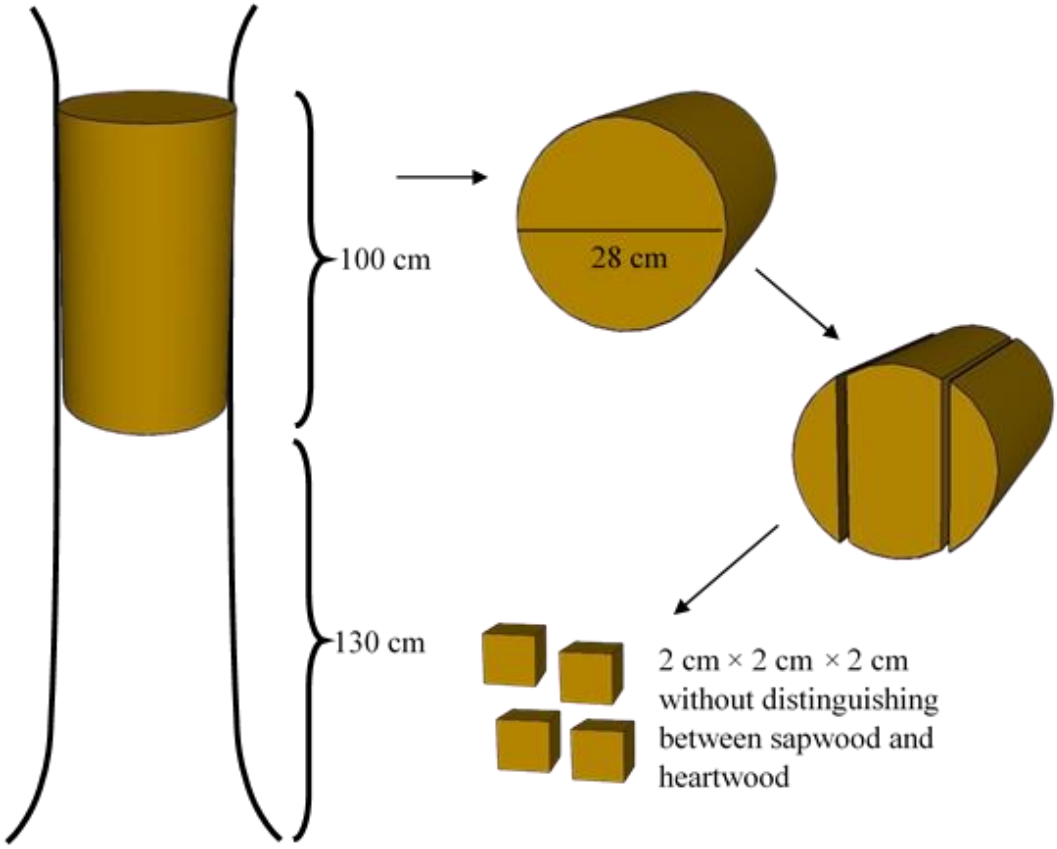

Fig. 1. Schematic illustration of the sampling and cutting pattern of sengon wood (*Falcataria moluccana*).

Table 1. Sample sizes for each test

Testing	Dimensions	Testing Standards
Weight percent gain (WPG), anti-swelling efficiency (ASE), water uptake (WU), bulking effect (BE), density, and leachability	2 cm × 2 cm × 2 cm (longitudinal × radial × tangential)	(BS 373:1957, 1999)

2.4. Synthesis of TiO_2 Nanoparticles

A 7 g sample of commercial bulk-phase TiO_2 powder was weighed and mixed with 75 mL of demineralized water. The mixture was placed in a steel autoclave (Andalan Lab Center, Lampung, Indonesia) and heated in an oven at 75 °C for 4 hours. The suspension was subjected to a low-temperature hydrothermal treatment to transform the bulk TiO_2 into nanosized particles and improve particle uniformity and surface reactivity before composite preparation. After that, the solution was cooled at room temperature for 24 hours. The resulting precipitate is then filtered and washed (Rahayu et al. 2022a).

2.5. Synthesis of SiO_2/TiO_2 Composite Nanoparticles

Weighting of SiO_2 and TiO_2 nanoparticles based on a 1:1 molar ratio. Weighed 1.5 g SiO_2 nanoparticles were mixed with 15 mL of NaOH 1 M solution (Selvakumar et al. 2014). A 3 g sample of TiO_2 nanoparticles was weighed and added to 60 mL of ethanol. Both solutions were mixed and sonicated (FS-250N, Henan Chuanghe Laboratory Equipment Co., Ltd., Henan, China) for 30 minutes to obtain a homogeneous suspension (Garskaite et al. 2019). The resulting mixture was placed in an autoclave (Andalan Lab Center, Lampung, Indonesia) and heated at 180 °C for 6 hours. Next, the mixed solution was washed with deionized water to remove unreacted precursors, thereby improving the crystallinity and stability of the composite nanoparticles (Ranjbar et al. 2015).

2.6. Preparation of Impregnation Solution

The solution mixture containing citric acid–glycerol (2:1) molar ratio and nanoparticles (SiO_2, TiO_2 and SiO_2/TiO_2 composite) was then processed by ultrasonication (FS-250N, Henan Chuanghe Laboratory Equipment Co., Ltd., Henan, China) at 40% amplitude for 2 hours. The concentration of the citric acid–glycerol solution was 20%, and each treatment mixture was prepared with 100 mL of demineralized water.

2.7. Nanoparticles Impregnation Process

Impregnation was carried out using the vacuum-press method (Rahayu et al. 2021). The test samples were first oven-dried at 103 ± 2 °C until the weight was constant. Subsequently, the impregnated specimens were weighed and measured. The ready test samples and impregnation solution were placed in the container inside the impregnation tube. The vacuum process was carried out first for 60 minutes at −0.5 bar gauge (approximately 0.5 bar absolute), followed by a press process for 120 minutes at 2.5 bar gauge. The impregnated samples were wrapped in foil and placed in an oven at 60 °C for 12 hours. Afterward, the test samples were placed in an oven at 103 ± 2 °C until they reached a constant weight.

2.8. Dimension Stability and Density Testing

Dimensional stability testing and density of impregnated sengon wood were carried out to determine the percentage value of weight percent gain (WPG), bulking effect (BE), and density (ρ). In addition, impregnated sengon wood was soaked to determine the anti-swelling efficiency (ASE) and water uptake (WU) (Rahayu et al. 2022a, 2022b). The calculation formulas used are given in Equations 1–5.

$$WPG\ (\%) = \frac{W_1 - W_0}{W_0} \times 100\ (\%) \quad (1)$$

where W_0 is the oven-dry weight of the sample before impregnation (g), and W_1 is the oven-dry weight of the sample after impregnation (g).

$$ASE\ (\%) = \frac{S_u - S_t}{S_u} \times 100\ (\%) \quad (2)$$

where S_u is the volumetric swelling of the control sample soaked in water at room temperature for 24 hours (cm^3), and S_t is the volumetric swelling of the sample that has been treated with impregnation (cm^3).

$$WU\ (\%) = \frac{W_2 - W_1}{W_1} \times 100\ (\%) \quad (3)$$

where W_1 is the oven-dry weight of the sample after impregnation (g), and W_2 is the weight of the sample after being immersed in water for 24 hours (g).

$$BE\ (\%) = \frac{V_1 - V_0}{V_0} \times 100\ (\%) \quad (4)$$

where V_0 is the oven-dry volume of the sample before impregnation treatment (cm^3), and V_1 is the oven-dry volume of the sample after impregnation treatment (cm^3).

$$\rho\ (g/cm^3) = \frac{B}{V} \quad (5)$$

where ρ is the density of the wood g/cm^3, B is the weight of the sample after impregnation treatment (g), and V is the volume of the sample after impregnation treatment (cm^3).

2.9. Characterization of Nanoparticles

Particle size analysis was performed using PSA. Test samples of SiO_2, TiO_2, and SiO_2/TiO_2 composite nanoparticles were sieved using a 100-mesh sieve. A 100 mL solution at 100 ppm was prepared. The solution was stirred using a magnetic stirrer for 20 minutes. That was applied as a pre-dispersion step to homogenize the suspension before analysis. Nanoparticle size analysis required 10 mL of the solution for 2–10 minutes. PSA measurements were conducted at room temperature (approximately 25 °C).

2.10. Characterization of Impregnated Sengon Wood

2.10.1. Fourier transform infrared spectroscopy

The untreated and impregnated samples were ground to 200 mesh and embedded in potassium bromide (KBr) pellets at a ratio of 1:100. The pellets were analyzed using a Perkin Elmer Spectrum One FTIR with a scanning range of 4000 to 400 cm^{-1} at a resolution of 4 cm^{-1} for 32 scans.

2.10.2. X-ray diffraction analysis

The wood sample was cut to a thickness of 2 mm in the tangential plane. The crystallinity level of the wood sample was analyzed using an XRD-PAN Analytical Empyrean type with a PIXcel 1D detector. The parameters used in the device were Cu Kα radiation with a graphite monochromator, a voltage of 40 kV, a current of 30 mA, and a scanning range of 0–50° at a scanning speed of 2°/minute. The degree of crystallinity (CrI) of wood samples was determined from X-ray diffraction (XRD) patterns using the Segal method, which is widely applied for lignocellulosic materials. The CrI was calculated from the intensity difference between the (200) crystalline cellulose plane at $2\theta \approx 22.5°$ and the amorphous region at $2\theta \approx 18°$, providing a relative measure of cellulose crystallinity in wood (Salem et al. 2023).

2.11. Data Analysis

Data analysis was performed using a completely randomized design and evaluated using ANOVA, followed by Duncan's multiple-range test at the 5% significance level ($\alpha = 0.05$). The analysis was conducted using IBM SPSS Statistics (Statistical Package for the Social Sciences) version 25.0. developed in Stanford, California, CA, USA.

3. Results and Discussion

3.1. Characteristics of Nanoparticles

3.1.1. Particle size analyzer (PSA) and zeta potential

Particle size analysis plays an important role in the impregnation process, ensuring its effectiveness and efficiency. Particles that are too large will have difficulty penetrating the wood structure and thus form only a surface layer. According to Nagraik et al. (2023), particles of 170 nm cannot efficiently penetrate the wood, whereas those of 70 nm can. Furthermore, in nanotechnology applications, particle size analysis is very important because it is related to effectiveness, stability, and quality control (Kastner and Perrie 2016). Detailed information regarding the particle size distribution of SiO_2 nanoparticles, TiO_2 nanoparticles, and SiO_2/TiO_2 composite nanoparticles can be seen in (**Fig. 2**).

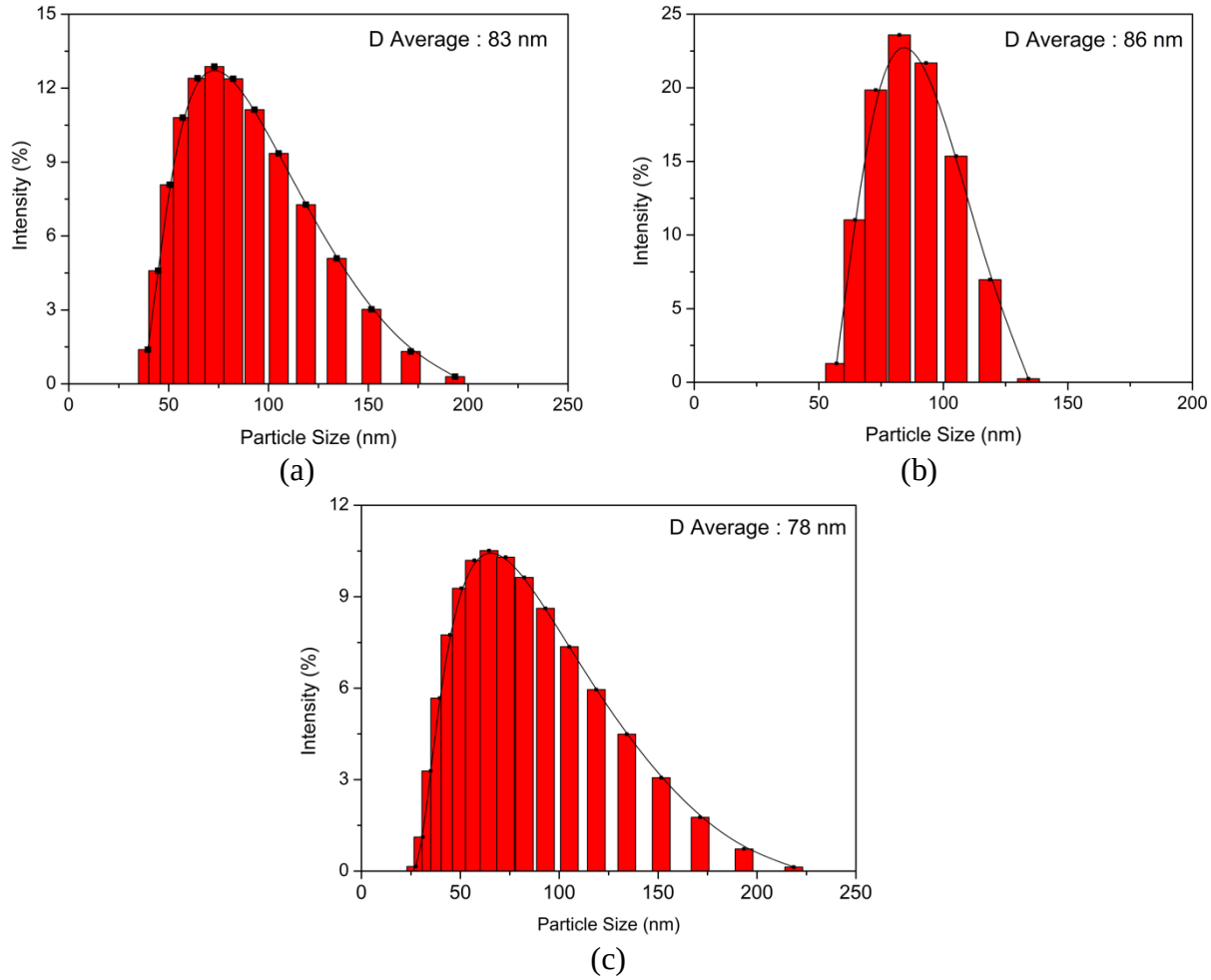

Fig. 2. The PSA analysis for the nanoparticles: (a) SiO_2 nanoparticles, (b) TiO_2 nanoparticles, and (c) SiO_2/TiO_2 composite nanoparticles.

The SiO_2 nanoparticles (**Fig. 2a**) obtained have a particle size distribution of approximately 39 nm–193 nm with an average particle size of 83 nm. The highest intensity was detected at 73 nm, and the lowest at 193 nm. The particles produced in this research are smaller than those in previous studies, which reported SiO_2 particle sizes of 52 µm and 207 nm, respectively (Haryono et al. 2018; Prihatini et al. 2024). TiO_2 nanoparticles (**Fig. 2b**) were identified in the particle size range of 57–134 nm, with an average of 86 nm. The particle size distribution exhibited a peak at approximately 82 nm and a valley at 134 nm. In contrast, Awad and Shaker (2021) reported an average particle size of 883 nm, which is larger than the value reported in this study. This significantly smaller particle size indicates that TiO_2 nanoparticles were successfully synthesized at low temperatures via a hydrothermal method, yielding uniform nanoscale particles with lower heat input (Hidayat et al. 2019).

The SiO_2/TiO_2 nanocomposite (**Fig. 2c**) revealed a particle size distribution in the range of 27 nm to 218 nm, with an average of 78 nm. The particle size distribution exhibits a unimodal profile, with a maximum at 64 nm. In comparison, particle sizes up to 218 nm correspond to the upper tail of the distribution rather than a secondary peak. According to the result of this PSA analysis, the nanoparticle synthesis was considered successful in maintaining an average particle size below 100 nm (83 nm for SiO_2, 86 nm for TiO_2, and 78 nm for the SiO_2/TiO_2 composite), although the particle size distributions indicate that some particles extend beyond 100 nm, reaching approximately 200–220 nm (Khan et al. 2019; Rachman et al. 2024).

The zeta potential analysis was conducted to assess particle stability, interactions, and behavior when dispersed in a commonly used solvent, water (Sikora et al. 2015). The stability of dispersed nanoparticles that form colloidal systems is proportional to their potential zeta value. A high potential zeta value indicates no agglomeration, and a low potential zeta value indicates an attractive force between particles that triggers particle agglomeration (Juliantoni et al. 2020). The zeta potential distribution shows a unimodal profile, with SiO_2 nanoparticles (**Fig. 3a**) exhibiting an average of −6.54 mV and a range of approximately −32.79 mV to 21.85 mV. The zeta potential of TiO_2 nanoparticles (**Fig. 3b**) has an average of −7.94 mV with a distribution range of approximately −38.08 mV to 16.67 mV. In addition to SiO_2 and TiO_2 nanoparticles, the zeta potential of SiO_2/TiO_2 composite nanoparticles (**Fig. 3c**) showed an average value of −38.94 mV with a distribution range of approximately −63.74 mV to −11.31 mV, indicating the overall distribution range rather than discrete intensity peaks.

The average zeta potential value of each nanoparticle shows that the stability of SiO_2 and TiO_2 nanoparticle dispersions is at a less stable level, so that the particles easily agglomerate, while SiO_2/TiO_2 composite nanoparticles produce dispersion stability at a stable level that makes the particles less prone to agglomeration. Generally, the zeta potential value can be said to have high stability when the value is greater than +30 mV or less than −30 mV (Dipahayu and Kusumo 2021; Zulfa et al. 2019). The negative zeta potential values obtained in this study are consistent with those reported by Sikora et al. (2015), which ranged from −10 mV to −50 mV, indicating negatively charged particle surfaces.

3.2. Dimensional Stability and Density of Sengon

Impregnation treatment using citric acid and glycerol solution (CA.G), CA.G–SiO_2 (CA.G–S) 1%, CA.G–TiO_2 (CA.G–T) 1%, CA.G–composite (CA.G–C) 1%, and water-composite (water–C) 1% showed their effectiveness in improving the dimensional stability of wood, as seen from

the increase in weight percent gain (WPG), anti-swelling efficiency (ASE), and bulking effect (BE) values. This treatment also contributed to an increase in wood density. All of these improvements are shown in **Fig. 4** to **Fig. 7.**

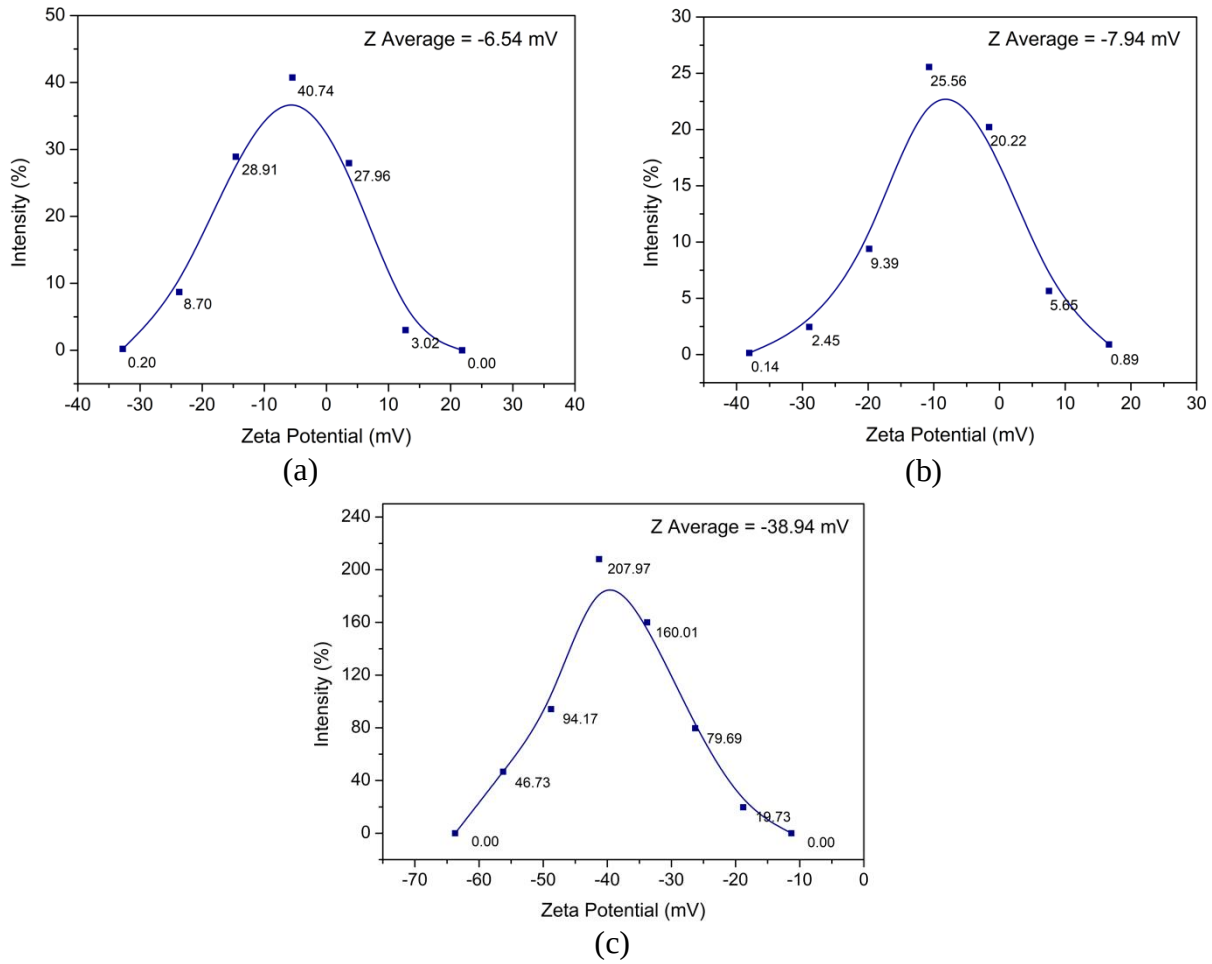

Fig. 3. Curves of zeta potential analysis: (a) SiO_2 nanoparticles, (b) TiO_2 nanoparticles, and (c) SiO_2/TiO_2 composite nanoparticles.

Fig. 4 shows that the highest WPG value was obtained for the CA.G–C 1% treatment on sengon wood, at 53.93%. This substantial weight gain occurs because citric acid and glycerol not only act as solvents but also as reactive agents capable of forming ester bonds with the –OH groups in the cellulose and hemicellulose of the wood cell wall, so that the modified material can bond chemically, not just physically fill the lumen or nodules (Essoua et al. 2016). Glycerol is also viscous and functions as a humectant, helping distribute SiO_2 and TiO_2 particles more evenly while reducing agglomeration, thereby improving diffusion into the wood tissue. Basri et al. (2024) also showed that non-biocide treatment with a mixture of citric acid, lactic acid, and glycerol on short-rotation teak wood can significantly increase WPG and wood density compared to the control.

The lowest value of 4.82% was observed for the 1% water–C treatment on sengon wood, as the use of water destabilized the SiO_2 and TiO_2 nanoparticles, leading to agglomeration and lower material retention in the wood. Statistical analysis shows that the WPG value of sengon wood is significantly influenced by the type of impregnation treatment with CA.G solution, SiO_2 nanoparticles, TiO_2 nanoparticles, and SiO_2/TiO_2 composite nanoparticles. Based on Duncan's further analysis, the water treatment of sengon wood is significantly different from that with CA.G. In addition, the polar nature of water tends to accelerate the agglomeration of SiO_2 and TiO_2

nanoparticles, preventing the particles from evenly entering the wood tissue (Liu et al. 2023). Xu et al. (2020) reported a maximum WPG of approximately 30% using a particle-free citric-acid-based modification system, in which chemical esterification contributed significantly to mass uptake. A more appropriate comparison can therefore be made with the particle-free citric acid–glycerol (CA.G) treatment used in the present study, which resulted in a WPG of 23.65%. In contrast, the water–particle system exhibited a much lower WPG (4.82%), reflecting the limited contribution of non-reactive water-based impregnation to overall mass gain.

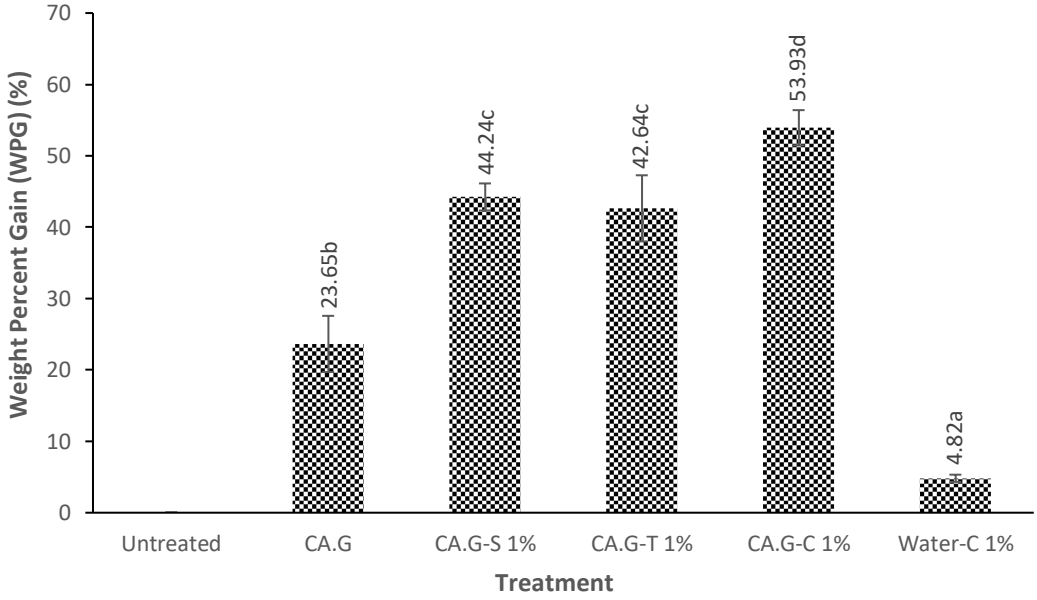

Fig. 4. Weight percent gain (WPG) of sengon wood across various impregnation treatments. Different letters above the bars indicate significant differences ($p < 0.05$) according to Duncan's post hoc test.

Fig. 5 indicates that the 1% G–C treatment achieved a maximum BE of 11.37% in sengon wood. Although the CA.G–C 1% treatment exhibited the highest BE value, it was not statistically different from the CA.G–S 1% treatment, indicating that adding TiO_2 to the SiO_2 system did not significantly improve bulking performance under the conditions studied. The high BE value for the 1% CA.G–C treatment likely resulted from the penetration of a blended mixture of citric acid, glycerol, and SiO_2/TiO_2 nanoparticles into the wood cells, with citric acid acting as a binder by forming ester linkages with hydroxyl groups on cellulose and hemicellulose. In contrast, glycerol acts as a co-reactant or softener, improving the physical interaction between chains to maintain a certain index of material stability within the cell wall (Essoua et al. 2016). Simultaneously, SiO_2 and TiO_2 nanoparticles are responsible for micropore filling and reinforcement of the structure of the wood cell wall. This dual mechanism is consistent with the study by Liu et al. (2023), which reported that a silica-impregnated composite resin can enhance the development effect by allowing particles to penetrate the wood cell walls. Furthermore, Essoua et al. (2016) explain that the use of citric acid and glycerol can increase material retention, resulting in a greater wood volume than when using a single solvent.

The lowest BE values were obtained in the untreated treatment on sengon wood at 1.19%, and in water–C 1% on sengon at 3.41%. The low BE values in the untreated and water–C 1% treatments occurred because water lacks functional groups that can react with wood components, so the filler is only physically retained in the pores and is easily washed out during drying.

Statistical analysis shows that the BE value of sengon wood is significantly influenced by the type of impregnation treatment with CA.G solution, SiO_2 nanoparticles, TiO_2 nanoparticles, and SiO_2/TiO_2 composite nanoparticles. Based on further Duncan analysis, untreated sengon wood differs significantly from wood treated with CA.G solution and nanoparticles. Additionally, the CA.G–C 1% treatment did not differ significantly from the CA.G–S 1% treatment.

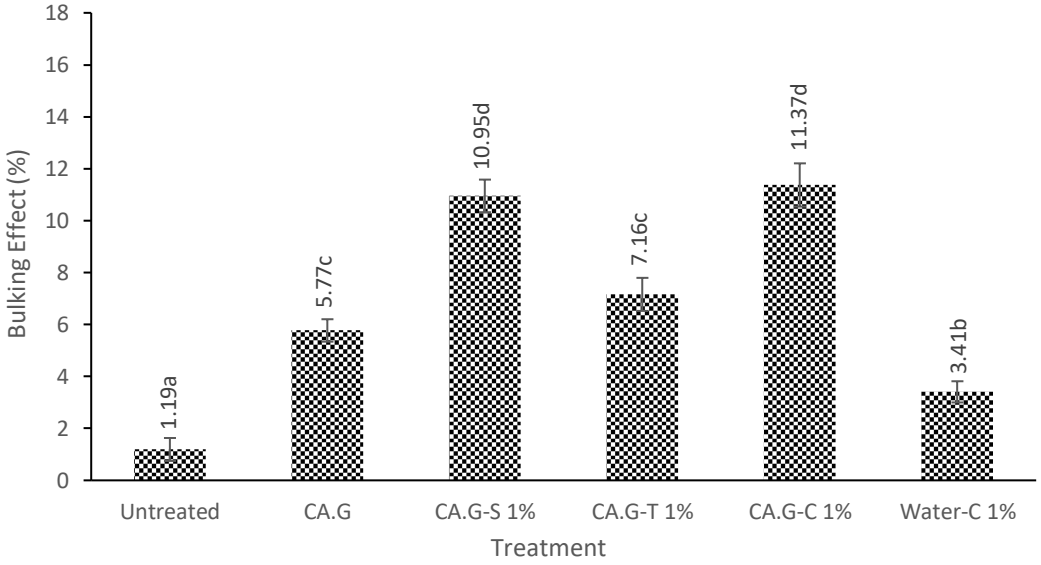

Fig. 5. Bulking effect (BE) of sengon wood across various impregnation treatments. Different letters above the bars indicate significant differences ($p < 0.05$) according to Duncan's post hoc test.

The use of water as a solvent tends to accelerate the agglomeration of SiO_2 and TiO_2 particles, which limits particle penetration into the cell wall (Essoua et al. 2016; Liu et al. 2023). As a result, the increase in wood volume from material deposition is relatively small, yielding a low BE value. The addition of impregnation solution, especially citric acid and glycerol, in this study caused the wood cell walls to expand and increased bulking in sengon wood, resulting in better dimensional stability. Thus, the wood maintained its dimensions, remaining unaffected by shrinkage or expansion, due to the treatment. According to Hill (2006), a higher BE value indicates that more polymers fill the wood cell cavities, thereby increasing dimensional stability.

Fig. 6 showed that the largest ASE value for sengon wood was also achieved with CA.G–C 1%; specifically, the percentages for the samples in the first, second, and third soaking-drying cycles were 80.21%, 67.37%, and 56.40%, respectively, showing distinct trends among the different impregnation treatments. The high ASE value in this treatment indicates that the synergistic effect between citric acid and glycerol with SiO_2 and TiO_2 nanoparticles can provide optimal protection of wood dimensional stability. This observation is consistent with that of L'Hostis et al. (2019), which also demonstrated that the ASE can increase by up to 64% for beech wood irradiated with citric acid and tartaric, attributed to the formation of stable chemical bonds on cell walls. Likewise, wood treatment with silica aerogels has resulted in an ASE value of 39.64% in the radial direction, due to the permanent swelling of wood cells (Bak et al. 2022). Furthermore, a preservative solution containing citric acid can even enhance the water resistance of the wood (Lee et al. 2020). Therefore, wood treated in this way is more resistant to decay even after several cycles of soaking and drying.

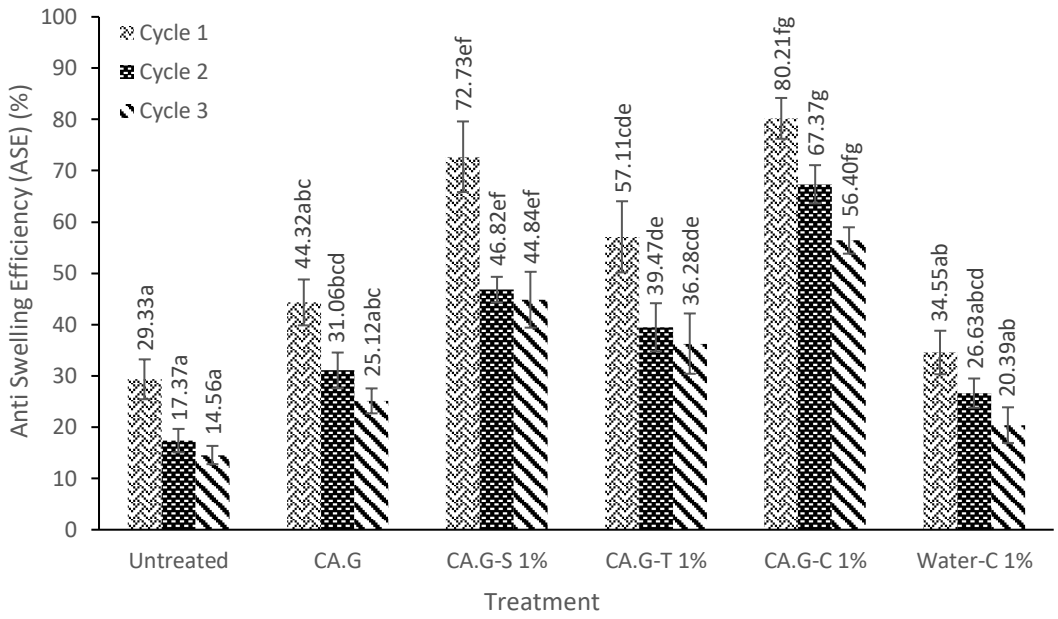

Fig. 6. Anti-swelling efficiency (ASE) of *sengon* wood across various impregnation treatments with 3 cycles. Different letters above the bars indicate significant differences ($p < 0.05$) based on Duncan's post hoc test.

The lowest ASE value was observed in the untreated sample, at only 29.33% in the first cycle and decreasing drastically to 14.56% in the third cycle. This low value is due to untreated wood still containing many free hydroxyl groups, which are highly hygroscopic and readily absorb water (Hill 2006). The low ASE in the water–C 1% treatment is consistent with Gómez et al. (2020), who found that water immersion can limit particle penetration through agglomeration, resulting in less effective pore filling and reduced chemical bonding to cell walls. Statistical analysis shows that the ASE value of sengon wood is significantly influenced by the type of impregnation treatment with CA.G solution, SiO_2 nanoparticles, TiO_2 nanoparticles, and SiO_2/TiO_2 composite nanoparticles. Based on further Duncan analysis, sengon wood without impregnation treatment differs significantly from that treated with CA.G solution and nanoparticles. In addition, the analysis of variance indicates that the cycle factor has no significant effect on the ASE value, and Duncan's test shows no difference.

Although two-way ANOVA indicated that the soaking–drying cycle factor did not have a statistically significant effect on ASE ($p > 0.05$), a clear decreasing trend in mean ASE values was observed across cycles. This statistical outcome is attributable to the relatively large standard deviation and to overlapping confidence intervals across cycles. The pronounced reduction in ASE during the initial cycle is likely due to leaching of physically deposited nanoparticles and unreacted citric acid–glycerol components during the first water immersion. Conversely, the remaining covalently bonded matrix contributes to the more stable ASE observed in subsequent cycles.

Fig. 7 shows that the CA.G–C 1% treatment achieved the highest density in sengon wood at 0.39 g/cm³, whereas the untreated treatment exhibited the lowest density at 0.29 g/cm³. Consistent with Augustina et al. (2023), these results confirm that impregnation successfully increases wood density. This improvement is largely driven by the use of citric acid, whose carboxyl groups interact with the wood's hydroxyl groups, thereby strengthening the overall structure (Larasati et al. 2017). Furthermore, Tobing et al. (2024) demonstrated that modification with both glycerol and citric acid significantly enhances density. This physical improvement occurs because the

modifying materials fill the lumens and cell walls, creating a denser and more compact internal structure.

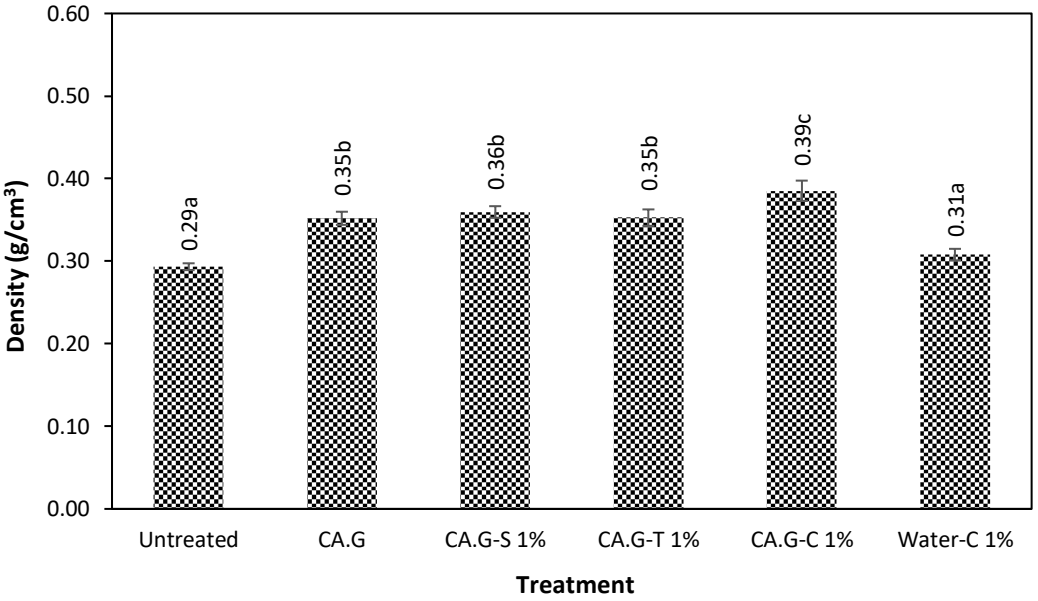

Fig. 7. Density of sengon wood across various impregnation treatments. Different letters above the bars indicate significant differences ($p < 0.05$) according to Duncan's post hoc test.

The addition of nanoparticles serves as a micropore filler, strengthening the wood structure (Essoua et al. 2016). Bowyer et al. (2007) stated that treatments that increase wood density are also associated with thicker wood cell walls. This increase in density indicates that the impregnation solution used in this study can effectively penetrate and fill the micro-pores in the wood cell wall, which, in turn, causes the cell wall to swell and become thicker (Hadiyane et al. 2018; Hill 2006). The density value of sengon wood was significantly influenced by the type of impregnation treatment with CA.G solution, SiO_2 nanoparticles, TiO_2 nanoparticles, and SiO_2/TiO_2 composite nanoparticles. Based on further Duncan analysis, the water treatment of sengon wood differs significantly from that added with CA.G solution, and the composite nanoparticle treatment differs significantly from other nanoparticle treatments.

The observed rise of WPG, density, BE, and ASE is accompanied by the drop in water uptake (WU) (**Fig. 8**). Reduced WU was observed on sengon wood following the treatment. This result reveals that treated wood exhibited greater resistance to water absorption from the environment into the wood substance. Simply put, wood is hygroscopic- it can take up and retain water. The highest WU value for sengon wood was observed in the untreated sample at 114.14%, whereas the lowest value was recorded for the CA.G–C 1% treatment at 59.16%, indicating that the SiO_2–TiO_2 composite effectively filled the wood pores and improved wood hydrophobicity. Our findings are analogous to those reported in (Liu et al. 2023) and (Sharma et al. 2022), which showed that organic acid impregnation-based soaking and silica nanoparticles effectively reduced wood water absorption by cross-linking and by particle deposition in the lumen. Liu et al. (2023) reported a 40% reduction in WU in poplar wood after impregnation with organic acids and nanoparticles, attributed to cross-link formation and particle deposition within the lumen.

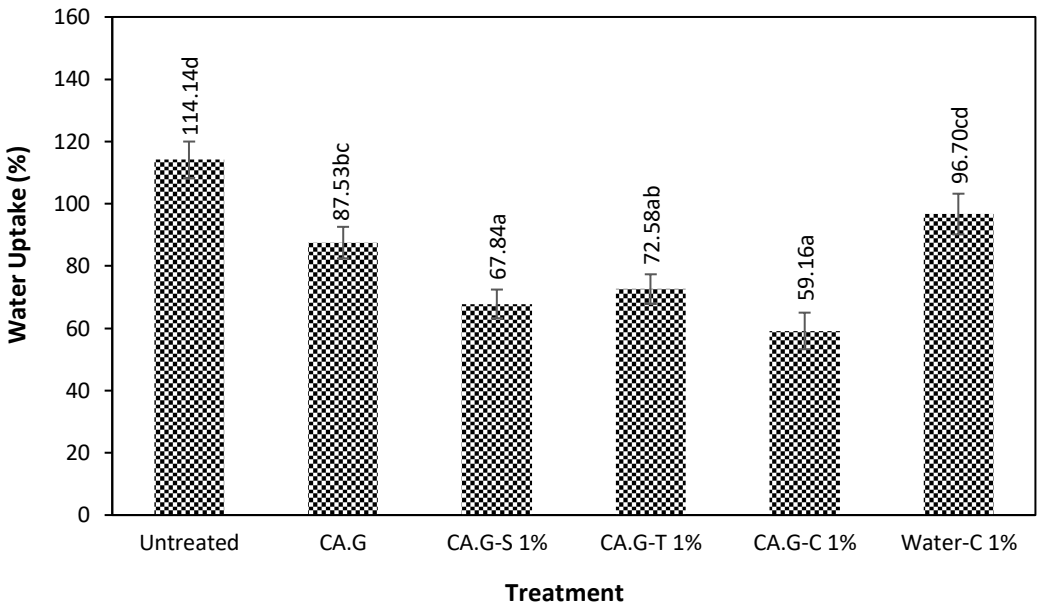

Fig. 8. Water uptake (WU) of sengon wood across various impregnation treatments. Different letters above the bars indicate significant differences ($p < 0.05$) according to Duncan's post hoc test.

The WU value decreased more with SiO_2 nanoparticle impregnation than with TiO_2 nanoparticle impregnation; however, the difference between the two treatments was not statistically significant. This is consistent with the work of Rahayu et al. (2025), which found that a TiO_2 coating on wood can greatly reduce water absorption and dimensional swelling. The study by Lemaire-Paul et al. (2023) shows that SiO_2 impregnation can also increase wood density and reduce porosity, leading to a lower WU value. The reduction in WU is attributed to the interaction of citric acid with cellulose and lignin in the wood, which decreases the availability of hydrophilic hydroxyl groups for moisture absorption. Statistical analysis revealed that impregnation with citric acid (CA) significantly reduced the WU of sengon wood. Furthermore, the addition of glycerol (G), SiO_2 nanoparticles, TiO_2 nanoparticles, and SiO_2/TiO_2 composite nanoparticles contributed to a further reduction in WU. Duncan's multiple range test confirmed that the water-impregnated sengon wood differed significantly from samples treated with CA.G solution and CA.G-based nanoparticle systems, whether applied as single or composite nanoparticle treatments ($p < 0.05$).

3.3. Characteristics of impregnated Sengon wood

3.3.1. Fourier transform infrared spectroscopy

Fourier transform infrared spectroscopy (FTIR) analysis (**Fig. 9**) was performed to identify functional groups present in untreated and treated sengon wood. The OH group peak of untreated sengon wood is at wavenumber 3272 cm^{-1} and lies within a fairly wide range. According to Kaygusuz (2019) and Rilda et al. (2020), extensive O–H absorption elongation vibrations occur in the range of 3600 cm^{-1} to 3100 cm^{-1}. In samples that underwent treatment, especially CA.G–C 1%, CA.G–T 1%, CA.G–S 1%, and CA.G, the wave numbers were 3417 cm^{-1}, 3414 cm^{-1}, 3414 cm^{-1}, and 3408 cm^{-1}, respectively. This wavenumber indicates low absorption intensity. The FTIR spectra of treated sengon wood showed distinct chemical changes compared with the untreated samples, confirming successful chemical modification. The broad O–H stretching band in the

region of 3200–3500 cm^{-1} decreased in intensity after CA.G-based treatments, which is attributed to esterification reactions between the modifying agents and the hydroxyl groups of cellulose, hemicellulose, and lignin. Rather than reflecting the mere presence of citric acid or glycerol, this esterification consumes free hydroxyl groups. Consequently, the reduced availability of hydroxyl groups limits the wood's ability to interact with water molecules, explaining why the treated wood absorbs less moisture than the untreated sample (Essoua et al. 2016).

The wavenumber at 2915 cm^{-1} in untreated sengon wood corresponds to the C–H stretching region (Rahayu et al. 2022a). The decrease in intensity in the treated wood indicates that the OH groups in cellulose and glycerol form esters, reducing the number of alkyl groups and thereby decreasing the C–H vibration intensity. Esterification introduces new carbonyl and ester C–O vibrations while consuming hydroxyl groups, but does not chemically consume alkyl (C–H) groups. Any apparent decrease in C–H band intensity is therefore more reasonably attributed to baseline shifting or peak overlap arising from the broad O–H and C=O absorption bands, rather than to the loss of C–H bonds (Lee et al. 2020).

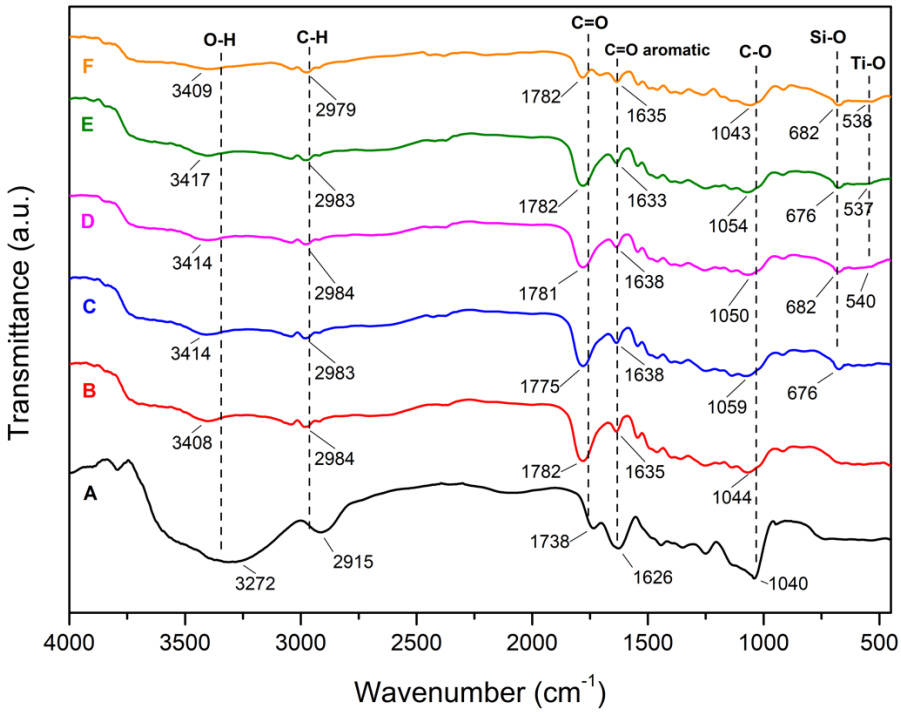

Fig. 9. FTIR analysis of sengon wood: untreated (A), CA.G (B), CA.G–S 1% (C), CA.G–T 1% (D), CA.G–C 1% (E), and Water–C 1% (F).

The wavenumbers 1738–1782 cm^{-1} correspond to the carbonyl (C=O) stretching band, and 377 cm^{-1} is consistent with ester bonds. The ester linkages are formed as a result of a polymerization reaction between glycerol and citric acid molecules, and the carboxylate group of the citric acid reacts with the hydroxyl group in wood (Essoua et al. 2016). For untreated sengon wood, a peak at 1738 cm^{-1} was assigned to the ester carbonyl groups of hemicellulose (Piqueras et al. 2020). In addition, the FTIR spectrum of wood samples treated with citric acid–glycerol showed high-intensity peaks at 1775–1782 cm^{-1}. This heightened intensity is attributed to the presence of citric acid anhydride (Cai et al. 2019) and reduced water adsorption.

A weak absorption band observed at approximately 1782 cm^{-1} is assigned to carbonyl (C=O) stretching vibrations, which may originate from ester or anhydride-like structures formed during

citric-acid-based esterification reactions (Lee et al. 2020). This band is not associated with SiO_2 or TiO_2 nanoparticles, as inorganic oxides typically exhibit characteristic vibrations in the lower wavenumber region below 1100 cm^{-1}. Therefore, the presence of this peak is more reasonably attributed to citric-acid-derived carbonyl functionalities within the modified wood matrix rather than to water-related effects or direct contributions from inorganic nanoparticles (Yang and Wöll 2017). The absorption band located at 1626–1639 cm^{-1} is primarily associated with the bending vibration of absorbed water in wood and overlaps with vibrations of conjugated carbonyl and carboxylate groups generated during citric-acid-induced esterification. Contributions from lignin aromatic skeletal vibrations may also occur in this region; therefore, this band should not be assigned exclusively to lignin C=O stretching, and the peak at wave numbers 1040 cm^{-1} is a stretching vibration of C–O and C–C functional groups of cellulose skeleton in wood (Freixas-Jambert et al. 2024).

The band around 1037 cm^{-1} corresponds mainly to C–O stretching vibrations of polysaccharides, particularly cellulose and hemicellulose. Although glycerol does not generate a unique FTIR peak, its participation in ester bond formation modifies the intensity and shape of this region through overlapping C–O–C and ester-related vibrations (Chen et al. 2018; Essoua et al. 2016). In the spectra of the treated wood, the intensity of this band decreases drastically, a reduction most likely driven by the addition of citric acid (Bernard et al. 2019; Essoua et al. 2016). The absorption peaks observed at approximately 676 cm^{-1} and 682 cm^{-1} are attributed to Si–O stretching vibrations, which are characteristic of silica-based structures. Similarly, the presence of TiO_2 is evidenced by absorption bands corresponding to Ti–O and Ti–O–Ti vibrational modes in the lower wavenumber region. These bands confirm the incorporation of silica- and titania-based components within the treated wood matrix (Prihatini et al. 2024). Meanwhile, FTIR analysis of samples impregnated with nano-TiO_2 also shows peaks at 546 cm^{-1}, 537 cm^{-1}, and 538 cm^{-1}. These wavenumbers correspond to Ti–O functional groups, which are consistent with the findings of Prihatini et al. (2024) and Rahayu et al. (2022a).

3.3.2. X-ray diffraction analysis

X-ray diffraction (XRD) analysis of sengon wood, treated and untreated with CA.G solution and nanoparticles using the impregnation method (**Fig. 10**), was conducted to observe changes in its characteristics, including the identification of crystal phases of impregnated nanoparticles and the degree of cellulose crystallinity in the wood. Untreated sengon wood exhibited three peaks at 2θ values of 15.32°, 22.22°, and 34.62°. The same peaks were identified in wood treated with CA.G solution and SiO_2 and TiO_2 nanoparticles, but with different intensities. These peak results are consistent with the research by Rahayu et al. (2022a), which identified the Miller indices at these peaks as (020), (012), and (131). Based on a comparison with the JCPDS No. 03-0226 standard cellulose diffractogram (Osman et al. 2019), these peaks were confirmed as cellulose, indicating that the crystal structure remained the same as in untreated wood. These findings indicate that the impregnation treatment did not have a significant effect on the cellulose phase of sengon wood, despite differences in intensity. Changes in peak intensity after citric acid–glycerol (CA.G) treatment reflect structural modification of the wood matrix rather than the removal of amorphous cellulose.

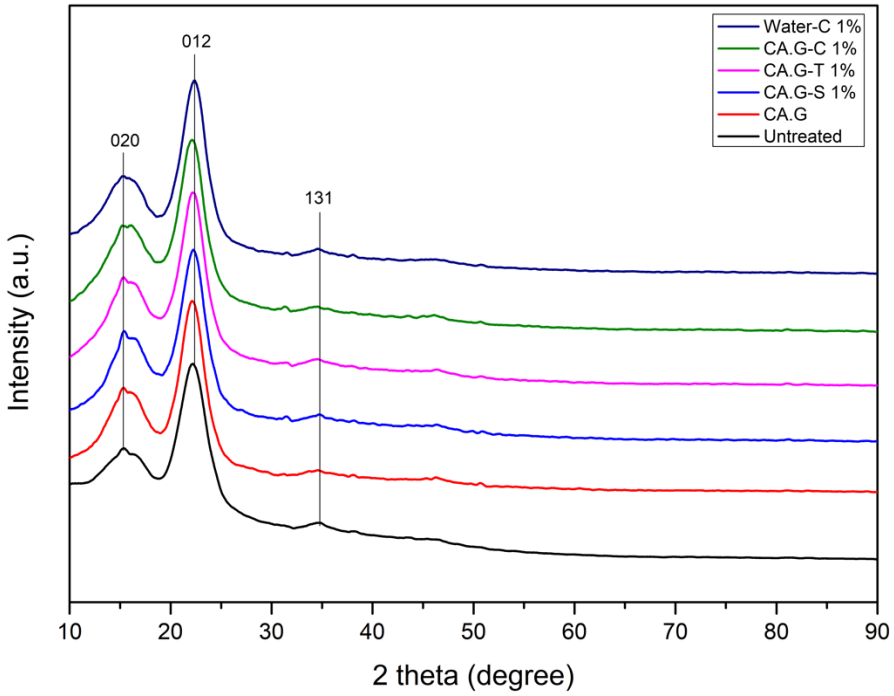

Fig. 10. Diffractogram of impregnated sengon wood.

Table 2. Degree of crystallinity of impregnated sengon wood

No	Treatment	Degree of Crystallinity (%)
1	Untreated	76.3
2	CA.G	51.0
3	CA.G–S 1%	42.4
4	CA.G–T 1%	42.1
5	CA.G–C 1%	43.3
6	Water–C 1%	46.8

The XRD analysis results show that sengon wood impregnated with the CA.G solution and nanoparticles exhibited decreased crystallinity (**Table 2**). The crystallinity of wood samples was evaluated using the Segal peak height method based on XRD data. The crystallinity index (CrI) was calculated using the intensity of the (012) crystalline plane ($I_{(012)}$) at approximately 22° and the intensity of the amorphous background (I_{am}) at approximately 18°. It should be noted that this method provides a relative crystallinity index rather than an absolute cellulose crystallinity value, and it may yield higher numerical values when applied to complex lignocellulosic systems. Consequently, the crystallinity values reported in this study are intended for comparative analysis between treatments, not as absolute measures of native cellulose crystallinity (Salem et al. 2023).

The highest crystallinity value in untreated sengon wood was 76.3%, while the lowest was in the CA.G–T 1% treatment, which was 42.1%. XRD analysis reflects the bulk crystalline lattice structure of cellulose within the wood matrix and is not influenced by surface wettability or hydrophobicity. While TiO_2 nanoparticles have been reported to improve wood hydrophobicity through micro-/nano-scale surface roughness, such surface phenomena do not affect XRD peak intensities or crystallinity indices. Therefore, any observed changes in crystallinity are attributed to chemical modification of the wood cell wall polymers and reorganization of crystalline and amorphous cellulose domains during impregnation and curing, rather than to surface

roughness-induced hydrophobic behavior (Cui and Li 2020). The decrease in crystallinity observed after CA.G treatment is attributed to the incorporation of a semi-crystalline/amorphous citric acid–glycerol polymer network within the wood structure. The presence of this polymer increases the proportion of amorphous regions relative to crystalline cellulose, thereby reducing the crystallinity index from 76.3% to 51.0%. Therefore, the XRD results indicate matrix dilution and disruption of cellulose crystalline order rather than removal of amorphous cellulose (Athanasoulia and Tarantili 2017).

4. Conclusions

The nanoparticles in this study were successfully synthesized with average particle sizes below 100 nm, despite a broader size distribution observed in the PSA results. SiO_2/TiO_2 composite nanoparticles have smaller particle sizes than SiO_2 and TiO_2, with the best particle stability that can minimize agglomeration, as indicated by the zeta potential value. Sengon wood treated by impregnation with a citric acid–glycerol solution and 1% SiO_2/TiO_2 composite nanoparticles (CA.G–C 1%) was the most effective in improving the physical properties and dimensional stability of the wood. This is demonstrated by an increase in wood density of 0.39 g/cm³, weight percent gain (WPG) of 53.93%, bulking effect (BE) of 11.37%, the highest anti-swelling efficiency (ASE) of 80.21% (cycle 1), and a decrease in water uptake (WU) by 59.16%. FTIR analysis confirmed the presence of chemical modification in the impregnated wood, evidenced by the formation of ester bonds that reduced free hydroxyl groups and decreased hydrophilicity. In addition, XRD analysis showed a decrease in the overall relative crystallinity in the treated wood, indicating that the amorphous impregnation polymer was successfully deposited and bound within the wood structure. Overall, sengon wood modified through (vacuum-pressure) impregnation with a combination of citric acid–glycerol and SiO_2/TiO_2 nanoparticle composites proved to be highly effective and has the potential to improve the quality of fast-growing wood.

Acknowledgments

This research is supported by the Directorate General of Research and Development, Ministry of Education, Science, and Technology of the Indonesian Government, in accordance with the Implementation Contract for the Research Program Fiscal Year 2025 Number 006/C3/DT.05.00/2025.

Author Contributions

S.: Formal Analysis, Investigation, Data Curation, Writing – Original Draft Preparation; I.S.R.: Conceptualization, Methodology, Validation, Investigation, Resources, Writing – Original Draft Preparation, Writing – Review and Editing, Supervision, Project Administration, Funding Acquisition; W.D.: Validation, Supervision, Writing – Review and Editing, Visualization; A.D.Y.: Validation, Investigation, Writing – Review and Editing, Supervision; E.P.: Methodology, Validation, Formal Analysis, Investigation, Data Curation, Writing – Original Draft Preparation, Visualization; G.D.L.: Methodology, Software, Formal Analysis, Investigation, Data Curation, Writing – Original Draft Preparation, Visualization, Writing – Review and Editing; R.I.: Methodology, Validation, Formal Analysis, Investigation, Data Curation, Writing – Original Draft Preparation, Visualization, Writing – Review and Editing.

Conflict of Interest

The authors declare no conflict of interest.

Declaration of Generative AI and AI-Assisted Technologies in the Manuscript Preparation

Not applicable.

References

Asci, Y., and Keskin, H. 2021. Strengthening the Retention Amount and Leaching Resistance of Boron Compounds Used as Impregnation Material. *Journal of Polytechnic* 24(1): 103–112. DOI: 10.2339/politeknik.687698

Athanasoulia, I., and Tarantili, P. 2017. Preparation and Characterization of Polyethylene Glycol/Poly(L-Lactic Acid) Blends. *Pure and Applied Chemistry* 89(1): 141–152. DOI: 10.1515/pac-2016-0919

Augustina, S., Dwianto, W., Wahyudi, I., Syafii, W., and Gérardin, P. 2023. Wood Impregnation in Relation to Its Mechanisms and Properties Enhancement. *BioResources* 18(2): 4332–4372. DOI: 10.15376/biores.18.2.4332-4372

Awad, S. H., and Shaker, F. 2021. Development of Self-Cleaning Bricks Surfaces by $CaCO_3$ Modified Nano-TiO_2 Composite Coatings. *Journal of Physics: Conference Series* 1973(1): 012142. DOI: 10.1088/1742-6596/1973/1/012142

Bak, M., Molnár, F., and Németh, R. 2018. Improvement of Dimensional Stability of Wood by Silica Nanoparticles. *Wood Material Science & Engineering* 14: 1–11. DOI: 10.1080/17480272.2018.1528568

Bak, M., Molnár, F., Rákosa, R., Németh, Z., and Németh, R. 2022. Dimensional Stabilization of Wood by Microporous Silica Aerogel Using In-Situ Polymerization. *Wood Science and Technology* 56(5): 1353–1375. DOI: 10.1007/s00226-022-01412-y

Basri, E., Rahayu, I. S., Saefudin, Santoso, A., Sulastiningsih, I. M., Damayanti, R., Martha, R., and Darmawan, W. 2024. Enhancement on Physicomechanical Properties of Short-Rotation Teak Woods by Non-Biocide Chemical and Thermal Treatments. *BioResources* 19(2): 3290–3305. DOI: 10.15376/biores.19.2.3290-3305

Belchinskaya, K. V., Zhukova, T. I., and Platonov, A. 2022. Impregnation of Wood with Waste Engine Oil to Increase Water- and Bio-Resistance. *Forests* 12(12): 1762. DOI: 10.3390/f12121762

Bernard, F., Rodrigues, D., Polesso, B., Chaban, V., Serevin, M., and Einloft, S. 2019. Development of Inexpensive Cellulose-Based Sorbents for Carbon Dioxide. *Brazilian Journal of Chemical Engineering* 36(1): 511–521. DOI: 10.1590/0104-6632.20190361s20170182

Bossert, D., Geers, C., Placencia Peña, M. I., Volkmer, T., Rothen-Rutishauser, B., and Petri-Fink, A. 2020. Size and Surface Charge Dependent Impregnation of Nanoparticles in Soft- and Hardwood. *Chemistry* 2(2): 361–373. DOI: 10.3390/chemistry2020023

Bowyer, J., Schmulsky, R., and Haygreen, J. 2007. *Forest Products and Wood Science: An Introduction*. 5th Edition. Iowa State Press.

BPS. 2022. *Statistik Produksi Kehutanan 2022*. Badan Pusat Statistik, Jakarta.

BPS. 2023. *Statistik Produksi Kehutanan 2022*. Badan Pusat Statistik, Jakarta.

BS 373:1957. 1999. *Methods of Testing Small Clear Specimens of Timber*. London.

Cahyani, I. S., Prasetya, A., and Purnomo, C. W. 2022. Nanosilica from Geothermal Sludge Using Sol-Gel Method with Addition of CTAB Surfactants. *AIP Conference Proceedings* 2391(1): 40004. DOI: 10.1063/5.0072886

Cai, Z., Ji, B., Yan, K., and Zhu, Q. 2019. Investigation on Reaction Sequence and Group Site of Citric Acid with Cellulose Characterized by FTIR in Combination with Two-Dimensional Correlation Spectroscopy. *Polymers* 11(12): 2071. DOI: 10.3390/polym11122071

Chen, Y., Lu, W., Guo, Y., Zhu, Y., Lu, H., and Wu, Y. 2018. Superhydrophobic Coatings on Gelatin-Based Films: Fabrication, Characterization and Cytotoxicity Studies. *RSC Advances* 8(42): 23712–23719. DOI: 10.1039/c8ra04066d

Cui, H., and Li, Q. 2020. Nano-Titanium Dioxide Coating of Chinese Fir Treated by High-Temperature Steam to Improve the Anticorrosion and Surface Hydrophobicity. *Forest Products Journal* 70(2): 158–164. DOI: 10.13073/fpj-d-19-00050

Dipahayu, D., and Kusumo, G. 2021. Formulasi dan Evaluasi Nano Partikel Ekstrak Etanol Daun Ubi Jalar Ungu (*Ipomoea batatas* L.) Varietas Antin-3. *Jurnal Sains dan Kesehatan* 3(6): 781–785. DOI: 10.25026/jsk.v3i6.818

Dong, Y., Yan, Y., Zhang, S., and Li, J. 2014. Wood/Polymer Nanocomposites Prepared by Impregnation with Furfuryl Alcohol and Nano-SiO_2. *BioResources* 9(2): 6028–6040. DOI: 10.15376/biores.9.4.6028-6040

Essoua, G. G. E., Blanchet, P., Landry, V., and Beauregard, R. 2016. Pine Wood Treated with a Citric Acid and Glycerol Mixture: Biomaterial Performance Improved by a Bio-Byproduct. *BioResources* 11(2): 3049–3072. DOI: 10.15376/biores.11.2.3049-3072

Freixas-Jambert, R., Ruiz-Recasens, C., Nieto-Villena, A., and Oriola-Folch, M. 2024. Non-Invasive Characterisation of Bromoil Prints by External Reflection FTIR Spectroscopy. *Molecules* 29(24): 5833. DOI: 10.3390/molecules29245833

Garskaite, E., Karlsson, O., Stankeviciute, Z., Kareiva, A., Jones, D., and Sandberg, D. 2019. Surface Hardness and Flammability of Na_2SiO_3 and Nano-TiO_2 Reinforced Wood Composites. *RSC Advances* 11(4): 27973–27986. DOI: 10.1039/c9ra05200c

Gómez, E. E. R., Hernández, J. H. M., and Astaiza, J. E. D. 2020. Development of a Chitosan/PVA/TiO_2 Nanocomposite for Application as a Solid Polymeric Electrolyte in Fuel Cells. *Polymers* 12(8): 1–14. DOI: 10.3390/polym12081691

Gürgen, A., and Yıldız, S. 2023. Some Physical and Biological Properties of *Pinus sylvestris* Wood Impregnated with Nano-Solutions. *Wood Industry and Engineering* 5(2): 10–17. DOI: 10.1007/ja37lk55pj

Hadiyane, A., Dungani, R., Dewi, S. P., and Rumidatul, A. 2018. Effect of Chemical Modification of Jabon Wood (*Anthocephalus cadamba* Miq.) on Morphological Structure and Dimensional Stability. *Journal of Biological Sciences* 18(4): 201–207. DOI: 10.3923/jbs.2018.201.207

Handayani, S. 2016. Analisis Pengujian Struktur Balok Laminasi Kayu Sengon Kayu Kelapa. *Jurnal Teknik Sipil dan Perencanaan* 18(1): 39–46. DOI: 10.15294/jtsp.v18i1.6693

Haryono, Rakhmawaty, D., Eddy, Noviyanti, A., Solihudin, and Laelaturrohmah. 2018. Kalsium Silikat Sebagai Bahan Komposit Biosemen Gigi dengan Penyiapan Silika dari Sekam Padi melalui Metode Sol-Gel. *Jurnal Kartika Kimia* 1: 5–10. DOI: 10.26874/jkk.v1i1.4

Hidayat, R., Fadillah, G., and Wahyuningsih, S. 2019. A Control of TiO_2 Nanostructures by Hydrothermal Condition and Their Application: A Short Review. *IOP Conference Series: Materials Science and Engineering* 578: 012031. DOI: 10.1088/1757-899x/578/1/012031

Hill, C. 2006. *Wood Modification. Chemical, Thermal and Other Processes*. John Wiley & Sons.

Horst, A., Neal, A., Mielke, R., Sislian, P., Suh, W., Madler, L., Stucky, G., and Holden, P. 2021. Dispersion of TiO_2 Nanoparticle Agglomerates by *Pseudomonas aeruginosa*. *Applied and Environmental Microbiology* 76(21): 7292–7298. DOI: 10.1128/aem.00324-10

Juliantoni, Y., Hajrin, W., and Subaidah, W. 2020. Nanoparticle Formula Optimization of Juwet Seeds Extract (*Syzygium cumini*) Using Simplex Lattice Design Method. *Jurnal Biologi Tropis* 20(3): 416–422. DOI: 10.29303/jbt.v20i3.2125

Kacíková, D., Kubovský, I., Eštoková, A., Kacík, F., Kmet'ová, E., Kováč, J., and Ďurkovič, J. 2021. The Influence of Nanoparticles on Fire Retardancy of Pedunculate Oak Wood. *Nanomaterials* 11: 3405. DOI: 10.3390/nano11123405

Kastner, E., and Perrie, Y. 2016. Particle Size Analysis of Micro and Nanoparticles. In: *Analytical Techniques in the Pharmaceutical Sciences*. Springer. 677–699. DOI: 10.1007/978-1-4939-4029-5_21

Kaygusuz, M. 2019. Sol-Gel Synthesis of TiO_2-SiO_2-Glymo Nanocomposite. *Journal of the Faculty of Engineering and Architecture of Gazi University* 49(2): 179–184.

Khan, I., Saeed, K., and Khan, I. 2019. Nanoparticles: Properties, Applications and Toxicities. *Arabian Journal of Chemistry* 12(7): 908–931. DOI: 10.1016/j.arabjc.2017.05.011

L'Hostis, C., Gérardin, P., Petithory, T., Gérardin-Charbonnier, C., and Pernes, M. 2019. Improvement of Beech Wood Properties by In Situ Formation of Polyesters of Citric and Tartaric Acid in Combination with Glycerol. *European Journal of Wood and Wood Products* 77: 913–924. DOI: 10.1007/s00266-019-01140-w

Larasati, D., Yuliasih, I., and Sunarti, T. 2017. Desain Proses Pembuatan Coating Film Berbasis Pati Sagu (*Metroxylon* sp.) Ikat Silang Asam Sitrat. *Jurnal Teknologi Industri Pertanian* 27(3): 318–327. DOI: 10.24961/j.tek.ind.pert.2017.27.3.318

Lee, S., Tahir, P., Lum, W., Tan, L., Bawon, P., Park, B., Al Edrus, S., and Abdullah, U. 2020. A Review on Citric Acid as Green Modifying Agent and Binder for Wood. *Polymers* 12(1692): 1–21. DOI: 10.3390/polym12081692

Lemaire-Paul, M., Beuthe, C. A., Riahinezhad, M., and Reza Foruzanmehr, M. 2023. The Impact of Vacuum Pressure on the Effectiveness of SiO_2 Impregnation of Spruce Wood. *Wood Science and Technology* 57(1): 147–171. DOI: 10.1007/s00226-022-01448-0

Liu, M., Li, X., Qin, Z., Liu, W., Li, C., and Le, L. 2023. Study on Modification of Poplar Wood Via Composite Impregnation with Silica Sol/Melamine–Glyoxal Resin. *Polymers* 15(21): 4247. DOI: 10.3390/polym15214247

Liu, X., Chen, S., and Fu, Y. 2021. Properties of *Pinus* Modified with Silicon-Titanium Binary Oxides. *BioResources* 16(1): 747–763. DOI: 10.15376/biores.16.1.747-763

Lu, Z., Hu, W., Xie, F., Zhuo, L., and Yang, B. 2017. Sol-Gel Synthesis of Nanosilica-Coated Para-Aramid Fibers and Their Application in the Preparation of Paper-Based Friction Materials. *RSC Advances* 7(49): 30632–30639. DOI: 10.1039/c7ra05142e

Manchanda, C. K., Khaiwal, R., and Mor, S. 2017. Application of Sol–Gel Technique for Preparation of Nanosilica from Coal Powered Thermal Power Plant Fly Ash. *Journal of Sol-Gel Science and Technology* 83(3): 574–581. DOI: 10.1007/s10971-017-4440-x

Mousa, E., and Taha, E. 2022. Synergetic Effects of Nanoparticle-SiO_2/Glycerol on the Electrical and Optical Properties of PVA for Embedded Electronics and Optical Applications. *Journal of Materials Science: Materials in Electronics* 33: 23088–23106. DOI: 10.1007/s10854-022-09075-y

Nagraik, P., Shukla, S. R., Kelkar, B. U., and Paul, B. N. 2023. Wood Modification with Nanoparticles Fortified Polymeric Resins for Producing Nano-Wood Composites: A Review. *Journal of the Indian Academy of Wood Science* 20(1): 1–11. DOI: 10.1007/s13196-023-00313-2

Osman, A. I., Blewitt, J., Abu-Dahrieh, J. K., Farrell, C., Al-Muhtaseb, A. H., Harrison, J., and Rooney, D. W. 2019. Production and Characterisation of Activated Carbon and Carbon Nanotubes from Potato Peel Waste. *Environmental Science and Pollution Research* 26(36): 37228–37241. DOI: 10.1007/s11356-019-06594-w

Piqueras, S., Füchtner, S., Rocha de Oliveira, R., Gómez-Sánchez, A., Jelavić, S., Keplinger, T., de Juan, A., and Thygesen, L. G. 2020. Understanding the Formation of Heartwood in Larch Using Synchrotron Infrared Imaging Combined with Multivariate Analysis and Atomic Force Microscope Infrared Spectroscopy. *Frontiers in Plant Science* 10: 01701. DOI: 10.3389/fpls.2019.01701

Prihatini, E., Laksono, G. D., Khairunissa, D., Rahayu, I., and Ismail, R. 2024. Characteristics and Applications of Bionanosilica from Betung Bamboo Leaves. *Journal of Engineering, Technology and Applied Science* 6: 153–166. DOI: 10.36079/lamintang.jetas-0603.766

Rachman, R. A., Wildan, M. W., and Fitriani, F. 2024. Sintesis dan Karakterisasi Nanosilika dari Limbah Silica Scaling PLTP Dieng Melalui Metode Alkali Fusion NaOH. *Journal of Mechanical Engineering* 1(1): 91–99. DOI: 10.47134/jme.v1i1.2194

Rahayu, I., Darmawan, W., Nawawi, D., Prihatini, E., Ismail, R., and Laksono, G. 2022a. Physical Properties of Fast-Growing Wood-Polymer Nano Composite Synthesized Through TiO_2 Nanoparticle Impregnation. *Polymers* 14(20): 4463. DOI: 10.3390/polym14204463

Rahayu, I., Darmawan, W., Zaini, L. H., and Prihatini, E. 2020. Characteristics of Fast-Growing Wood Impregnated with Nanoparticles. *Journal of Forestry Research* 31(2): 677–685. DOI: 10.1007/s11676-019-00902-3

Rahayu, I., Pratama, A., Darmawan, W., Nandika, D., and Prihartini, E. 2021. Characteristic of Impregnated Wood by Nanoparticle Silica from Betung Bamboo Leaves. *IOP Conference Series: Earth and Environmental Science* 891: 012019. DOI: 10.1088/1755-1315/891/1/012019

Rahayu, I., Prihatini, E., Ismail, R., Darmawan, W., Karlinasari, L., and Laksono, G. 2022b. Fast-Growing Magnetic Wood Synthesis by an In-Situ Method. *Polymers* 14(11): 2137. DOI: 10.3390/polym14112137

Ranjbar, M., Taher, M., and Sam, A. 2015. Single-Step Synthesis of SiO_2-TiO_2 Hydrophobic Core-Shell Nanocomposite by Hydrothermal Method. *Journal of Cluster Science* 27(2): 583–592. DOI: 10.1007/s10876-015-0953-z

Rilda, Y., Dwiyanti, D., Syukri, S., Agustien, A., and Pardi, H. 2020. Enhancement of Antifungal Capability of Cotton Textiles Coated with TiO_2–SiO_2/Chitosan Using Citric Acid and Sodium Hypophosphite Catalyst. *Journal of Dispersion Science and Technology* 42(5): 784–790. DOI: 10.1080/01932691.2020.1724797

Rosales, A., and Esquivel, K. 2020. SiO_2@TiO_2 Composite Synthesis and Its Hydrophobic Applications: A Review. *Catalysts* 10(2): 171. DOI: 10.3390/catal10020171

Salem, K. S., Kasera, N. K., Rahman, M. A., Jameel, H., Habibi, Y., Eichhorn, S. J., French, A. D., Pal, L., and Lucia, L. A. 2023. Comparison and Assessment of Methods for Cellulose Crystallinity Determination. *Chemical Society Reviews* 52(18): 6417–6446. DOI: 10.1039/d2cs00569g

Saputra, A. R., Alimuddin, and Julia, R. R. D. 2017. Sintesis Material Silika Mesopori SBA-15 dari Abu Daun Bambu Petung (*Dendrocalamus asper* (Schult.) Backer Ex Heyne) dan Pemanfaatannya sebagai Adsorben Metilen Biru. *Prosiding Seminar Nasional Kimia 2017*: 106–110.

Selvakumar, K. V., Umesh, A., Ezhilkumar, P., Gayatri, S., Vinith, P., and Vignesh, V. 2014. Extraction of Silica from Burnt Paddy Husk. *International Journal of ChemTech Research* 6(9): 4455–4459. URL: https://sphinxsai.com/2014/rtbce/6/(4455-4459)%20014.pdf

Sharma, P., Prakash, J., and Kaushal, R. 2022. An Insight into the Green Synthesis of SiO_2 Nanostructures as a Novel Adsorbent for Removal of Toxic Water Pollutants. *Environmental Research* 212(Part C): 113328. DOI: 10.1016/j.envres.2022.113328

Sikora, A., Bartczak, D., Geißler, D., Kestens, V., Roebben, G., Ramaye, Y., Varga, Z., Palmai, M., Shard, A. G., Goenaga-Infante, H., and Minelli, C. 2015. A Systematic Comparison of Different Techniques to Determine the Zeta Potential of Silica Nanoparticles in Biological Medium. *Analytical Methods* 7(23): 9835–9843. DOI: 10.1039/c5ay02014j

Tobing, G., Sofiaturizkiyah, N., Basri, E., Martha, R., Rahayu, I., Gérardin, P., and Darmawan, W. 2024. Mikrostruktur dan Karakteristik Permukaan Kayu Pinus Scots (*Pinus sylvestris* L.) Termodifikasi Gliserol dan Asam Sitrat. *Jurnal Ilmu Pertanian Indonesia* 29(4): 554–563. DOI: 10.18343/jipi.29.4.554

Xu, E., Zhang, Y., and Lin, L. 2020. Improvement of Mechanical, Hydrophobicity and Thermal Properties of Chinese Fir Wood by Impregnation of Nano Silica Sol. *Polymers* 12(8): 1632. DOI: 10.3390/polym12081632

Yang, C., and Wöll, C. 2017. IR Spectroscopy Applied to Metal Oxide Surfaces: Adsorbate Vibrations and Beyond. *Advances in Physics: X* 2(2): 373–408. DOI: 10.1080/23746149.2017.1296372

Zulfa, E., Novianto, D., and Setiawan, D. 2019. Diclofenac Sodium Nanoemulsion Formulation with Tween 80 and Span 80 Combination Variations: Study of Physical Characteristics of Preparations. *Indonesian Pharmaceutical Media* 14(1): 1471–1477.